Defining Maximum and Minimum Transverse Regions to Study the Underlying Event in Hard Scattering Processes

Rick Field, Richard Haas, and David Stuart

May 7, 2001

Abstract

We use the direction of the leading charged particle jet in each event to define a "transverse" region of η-ϕ space that is very sensitive to the "underlying event" in hard scattering processes. This "transverse" region is then separated into its maximum ("transMAX") and minimum ("transMIN") pieces. The various components that make up the underlying event are weighted differently in the "transMAX" and "transMIN" terms. The "transMAX" term preferentially selects the hard component of the underlying event (outgoing jets plus initial and final-state radiation) while the "transMIN" term preferentially selects the beam-beam remnant component. Requiring the QCD hard scattering Monte-Carlo models to fit both "transMAX" and "transMIN" (or the sum and difference) puts additional constraints on the way the generators model the underlying event.

I. Introduction

In a proton-antiproton collision a large transverse momentum outgoing parton manifests itself in the laboratory as a cluster of particles (*both charged and neutral*) traveling in roughly the same direction. These clusters are referred to as "jets". This is an extension of our previous work [1] where we examine only the charged particle component of "jets". Using a simple algorithm, we study clusters of charged particles which we call "charged particle jets". The transverse momentum of the "charged particle jet" is the sum of the transverse momentums of the charged particles making up the "jet". We use the direction of the leading charged particle jet in each event to define a "transverse" region of η-ϕ space that is very sensitive to the "underlying event". In this analysis, we separate this "transverse" region into its maximum and minimum pieces in order to further isolate the components of the "underlying event" in hard scattering processes.

A hard scattering event, like that illustrated in Fig. 1.1 consists of large transverse momentum outgoing hadrons that originate from the large transverse momentum partons (*i.e.* outgoing hard scattering jets) and also hadrons that originate from the break-up of the proton and antiproton (*i.e.* the "beam-beam remnants"). The underlying event is an interesting object that is not very well understood. In addition to beam-beam remnants, it may contain hadrons resulting from initial-state radiation. Also, it is possible that multiple parton scattering contributes to the underlying event. PYTHIA , for example, uses multiple parton interactions as a way to enhance the activity of the underlying event [2].

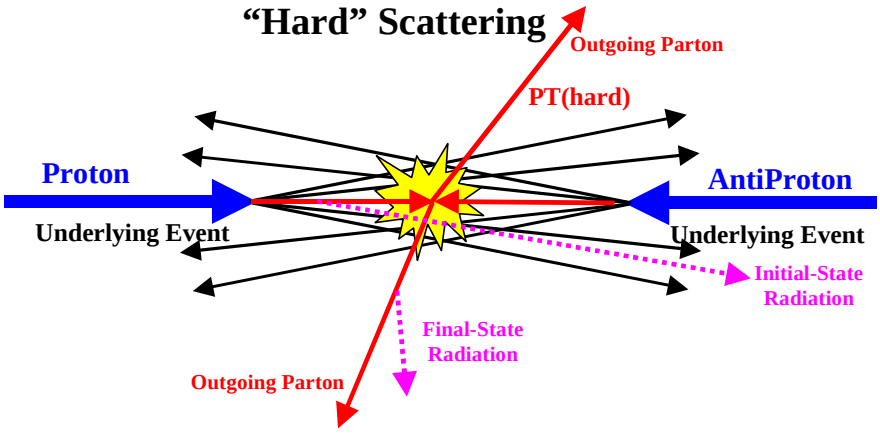

Fig. 1.1. Illustration of a proton-antiproton collision in which a "hard" 2-to-2 parton scattering with transverse momentum, P_T(hard), has occurred. The resulting event contains particles that originate from the two outgoing partons (plus final-state radiation) and particles that come from the breakup of the proton and antiproton (*i.e.* "beam-beam remnants"). The "underlying event" consists of the beam-beam remnants plus initial and final-state radiation.

We discuss the data analysis in Section II and in Section III we review our study of the "transverse" region and the underlying event. Section II and Section III are from our previous work [1]. In Section IV we present new results on the maximum and minimum "transverse" regions and compare with the QCD hard scattering Monte-Carlo models. We reserve Section V for summary and conclusions.

II. Data Selection

As in our previous work [1] we consider only charged particles measured in the central tracking chamber (CTC) and use the two trigger sets of data listed in Table 1. To reduce the contribution spurious tracks that result from secondary interactions between primary particles, including neutral particles, and the detector material, we consider only tracks which point to the primary interaction vertex within 2 cm along the beam direction and 1 cm transverse to the beam direction. Detector simulations indicate that this impact parameter cut is very efficient and that the number of spurious tracks is about 3.5% when a 1 cm impact parameter cut is applied in conjunction with a 2 cm vertex cut. Without the impact parameter cut the number of spurious tracks is approximately 9%.

This dependence of the number of spurious tracks on the CTC impact parameter cut provides a method of estimating systematic uncertainties due to unwanted (*i.e.* fake) tracks. Every data point on every plot in this analysis was determined three times by using a 2 cm vertex cut in conjunction with three different CTC d_0 cuts: a 1 cm CTC d_0 cut; a 0.5 cm CTC d_0 cut; and no CTC d_0 cut. The 1 cm cut determined the value of the data point and the difference between the 0.5 cm cut value and the no cut value of the data point was used to estimate the systematic error. This systematic error was then added in quadrature with the statistical error. We do not correct the data for the CTC track finding efficiency. Instead the theoretical Monte-Carlo model predictions are corrected for the track finding efficiency. These corrections are small (less than 10%).

Table 1. Data sets and selection criterion used in this analysis.

CDF Data Set	Trigger	Events	Selection
Min-Bias	Min-Bias Trigger	626,966	zero or one vertex in $\|z\| < 100$ cm $\|z_c - z_v\| < 2$ cm, $\|$CTC $d_0\| < 1$ cm $P_T > 0.5$ GeV/c, $\|\eta\| < 1$
JET20	Calorimeter tower cluster with $E_T > 20$ GeV/c	78,682	zero or one vertex in $\|z\| < 100$ cm $\|z_c - z_v\| < 2$ cm, $\|$CTC $d_0\| < 1$ cm $P_T > 0.5$ GeV/c, $\|\eta\| < 1$

Our philosophy in comparing the QCD Monte-Carlo models with data is to select a region where the data is very "clean". The CTC efficiency can vary substantially for very low P_T tracks and in dense high P_T jets. To avoid this we have considered only the region $P_T > 0.5$ GeV/c and $|\eta| < 1$ where the CTC efficiency is high and stable (estimated to be 92% efficient) and we restrict ourselves to charged particle jets less than 50 GeV/c. The data presented here are uncorrected. Instead the theoretical Monte-Carlo models are corrected for the track finding efficiency. In this analysis we use PYTHIA 6.115 [2], HERWIG 5.9 [3], and ISAJET 7.32 [4] with the default parameters for each and take P_T(hard) > 3 GeV/c. The errors on the (*uncorrected*) data include both statistical and correlated systematic uncertainties.

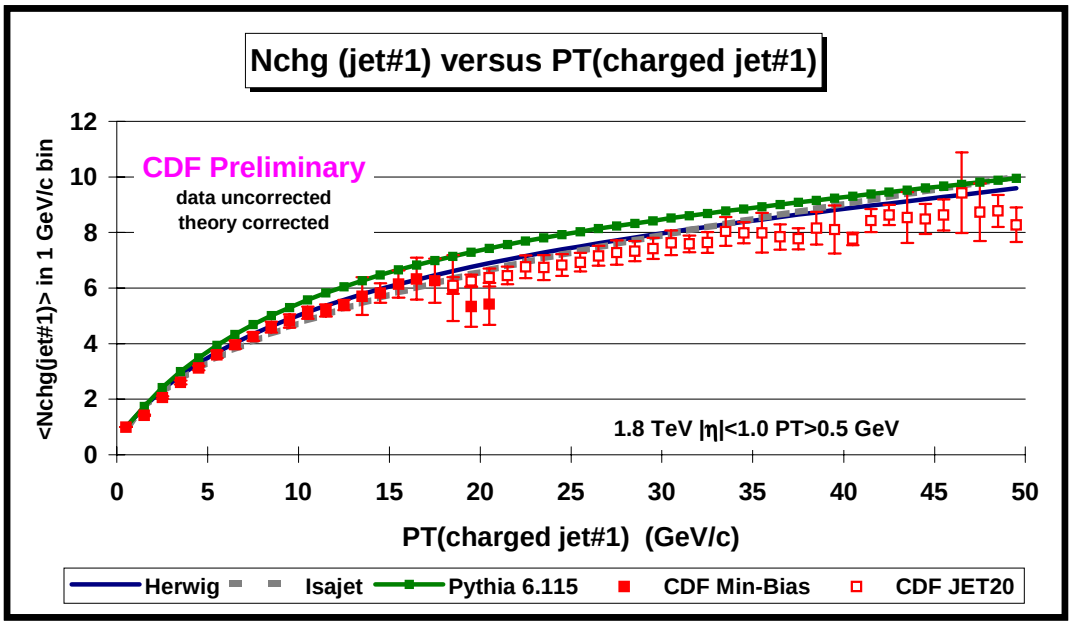

Fig. 3.1. Plot shows the average number of charged particles ($P_T > 0.5$ GeV/c, $|\eta| < 1$) within the leading charged jet (R = 0.7) as a function of the P_T of the leading charged jet. The solid (open) points are Min-Bias (JET20) data. The errors on the (*uncorrected*) data include both statistical and correlated systematic uncertainties. The QCD hard scattering theory curves (HERWIG, ISAJET, PYTHIA 6.115) are corrected for the track finding efficiency and have an error (*statistical plus systematic*) of around 5%.

III. The "Transverse" Region and the Underlying Event

Charged particle jets are defined as clusters of charged particles ($P_T > 0.5$ GeV/c, $|\eta| < 1$) in "circular regions" of η-ϕ space with radius R = 0.7. The jets contain charged particles from the underlying event as well as particles which originate from the fragmentation of high P_T outgoing partons (see Fig 1.1). Also every charged particle in the event is assigned to a jet, with the possibility that some jets might consist of just one charged particle. Fig. 3.1 shows the average number of charged particles within chgjet#1 *(leading charged jet*) as a function of P_T(chgjet#1). The solid points are Min-Bias data and the open points are the JET20 data. The JET20 data connect smoothly to the Min-Bias data and allows us to study observables over the range $0.5 < P_T$ (chgjet#1) < 50 GeV/c. There is a small overlap region where the Min-Bias and JET20 data agree. Of course, if we had a larger sample of Min-Bias data, it would contain the JET20 data. The data are compared with the QCD hard scattering Monte-Carlo predictions of HERWIG, ISAJET, and PYTHIA.

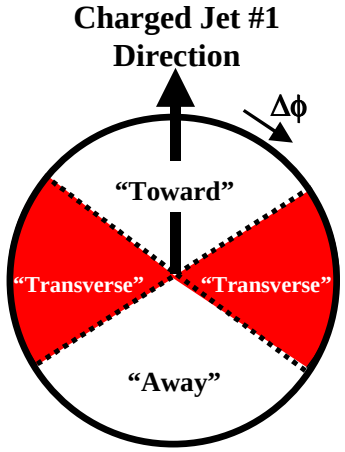

Fig. 3.2. Illustration of correlations in azimuthal angle $\Delta\phi$ relative to the direction of the leading charged jet in the event, chgjet#1. The angle $\Delta\phi = \phi - \phi_{chgjet\#1}$ is the relative azimuthal angle between charged particles and the direction of chgjet#1. The "transverse" region is defined by $60^o < |\Delta\phi| < 120^o$ and has an area in η-ϕ space of $\Delta\eta \times \Delta\phi = 2 \times 120^o$.

The "transverse" region defined in Fig. 3.2 is roughly normal to plane of the 2-to-2 hard scattering and is therefore very sensitive to the underlying event. Fig. 3.3 and Fig. 3.4 compare the "transverse" $\langle N_{chg} \rangle$ and the "transverse" $\langle PT_{sum} \rangle$, respectively, with the QCD hard scattering Monte-Carlo predictions. Fig. 3.3 shows that the average number of charged particles in the "transverse" region doubles in going from P_T(chgjet#1) = 1.5 GeV/c to P_T(chgjet#1) = 2.5 GeV/c and then forms an approximately constant "plateau" for P_T(chgjet#1) > 5 GeV/c.

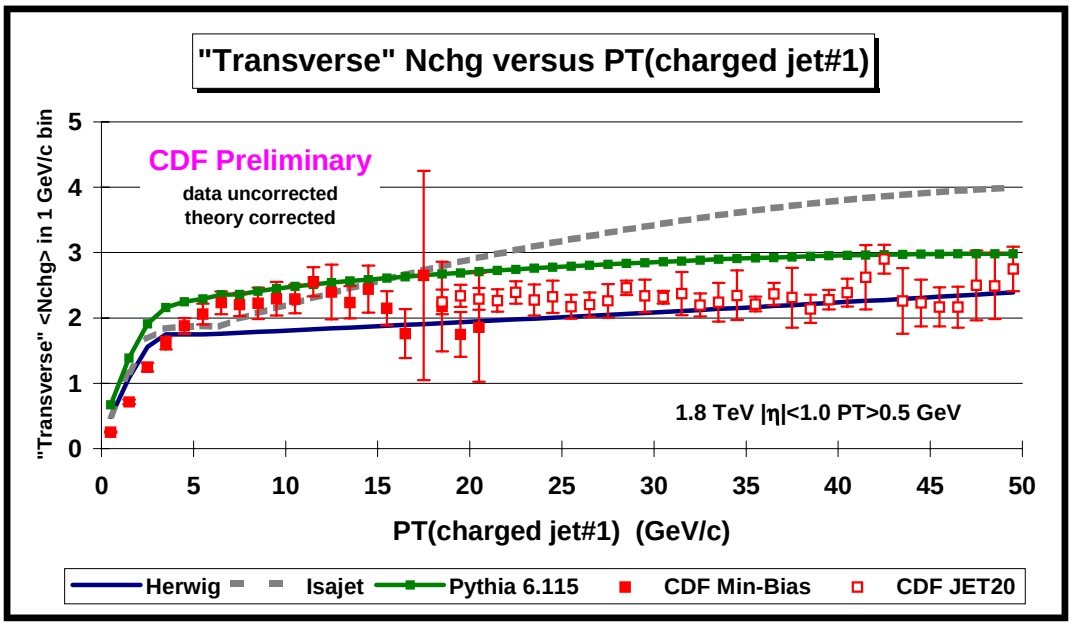

Fig. 3.3. Data on the average number of charged particles (P_T > 0.5 GeV/c and |η| < 1) as a function of P_T(chgjet#1) (*leading charged jet*) for the "transverse" region defined in Fig. 3.2 compared with the QCD hard scattering Monte-Carlo predictions of HERWIG, ISAJET, and PYTHIA 6.115. Each point corresponds to the <Nchg> in a 1 GeV/c bin. The solid (open) points are the Min-Bias (JET20) data. The errors on the (*uncorrected*) data include both statistical and correlated systematic uncertainties. The theory curves are corrected for the track finding efficiency and have an error (*statistical plus systematic*) of around 5%.

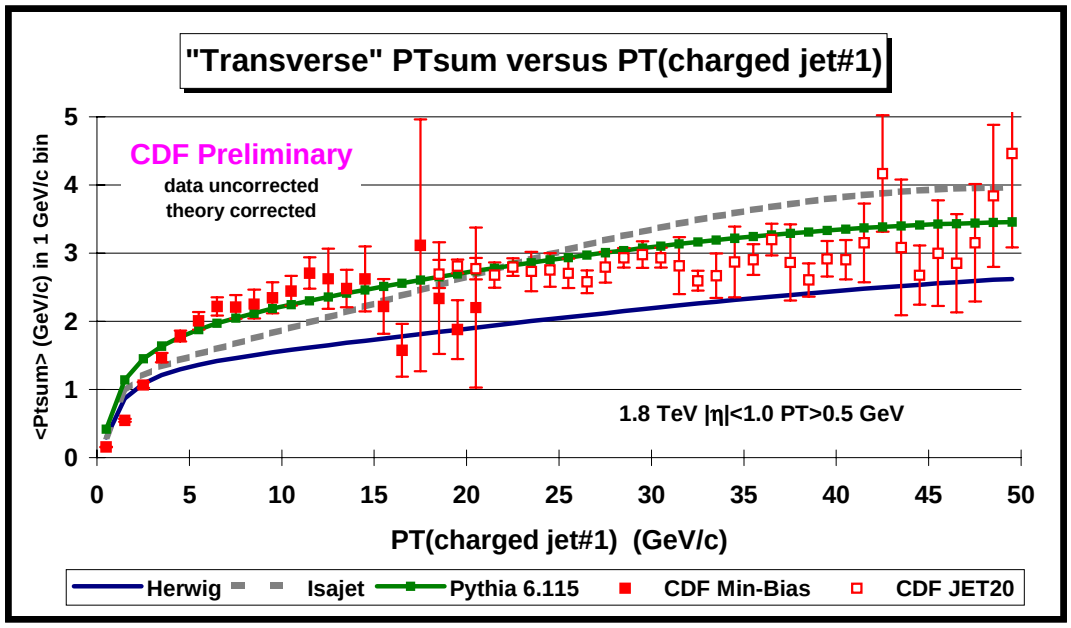

Fig. 3.4. Data on the average *scalar* P_T sum of charged particles (P_T > 0.5 GeV/c and |η| < 1) as a function of P_T(chgjet#1) (*leading charged jet*) for the "transverse" region defined in Fig. 3.2 compared with the QCD hard scattering Monte-Carlo predictions of HERWIG, ISAJET, and PYTHIA 6.115. Each point corresponds to the <PTsum> in a 1 GeV/c bin. The solid (open) points are the Min-Bias (JET20) data. The errors on the (*uncorrected*) data include both statistical and correlated systematic uncertainties. The theory curves are corrected for the track finding efficiency and have an error (*statistical plus systematic*) of around 5%.

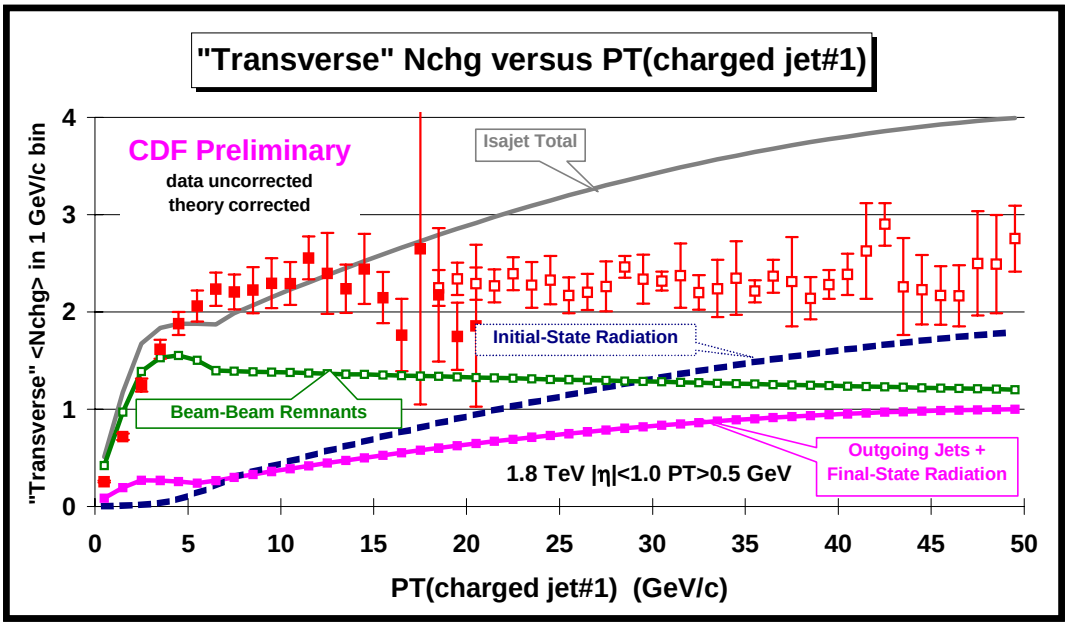

Fig. 3.5. Data on the average number of charged particles (P_T > 0.5 GeV/c and |η| < 1) as a function of P_T(chgjet#1) (*leading charged jet*) for the "transverse" region defined in Fig. 3.2 compared with the QCD hard scattering Monte-Carlo predictions of ISAJET. The predictions of ISAJET are divided into three categories: charged particles that arise from the break-up of the beam and target (*beam-beam remnants*), charged particles that arise from initial-state radiation, and charged particles that result from the outgoing jets plus final-state radiation (see Fig. 1.1). The theory curves are corrected for the track finding efficiency and have an error (*statistical plus systematic*) of around 5%.

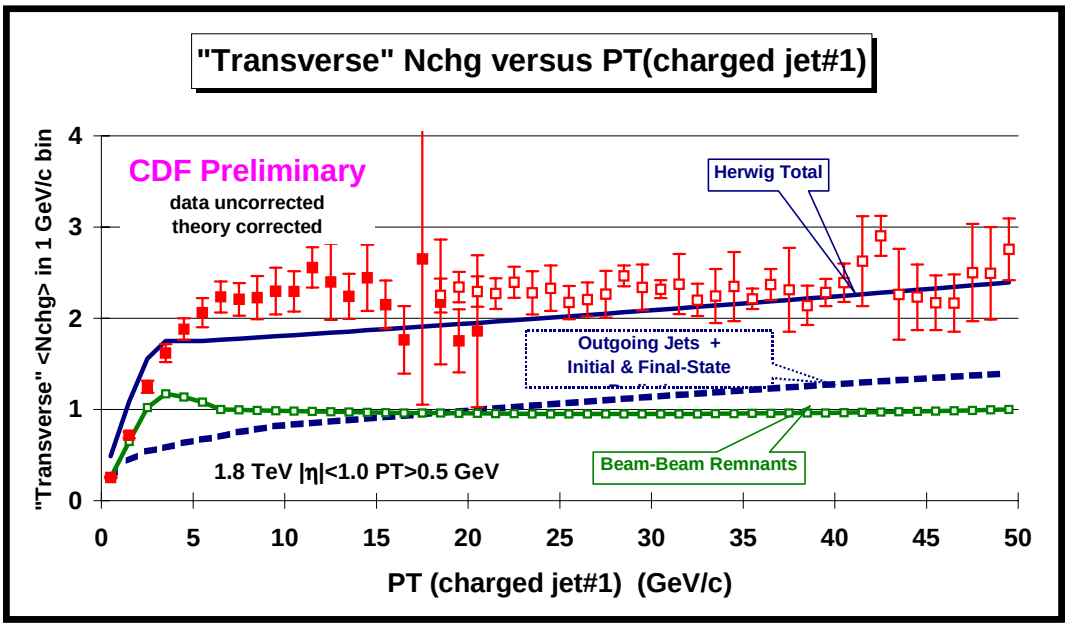

Fig. 3.6. Data on the average number of charged particles (P_T > 0.5 GeV/c and |η| < 1) as a function of P_T(chgjet#1) (*leading charged jet*) for the "transverse" region defined in Fig. 3.2 compared with the QCD "hard scattering" Monte-Carlo predictions of HERWIG. The predictions of HERWIG are divided into two categories: charged particles that arise from the break-up of the beam and target (*beam-beam remnants*), and charged particles that result from the outgoing jets plus initial and final-state radiation (*hard scattering component*) (see Fig. 1.1). The theory curves are corrected for the track finding efficiency and have an error (*statistical plus systematic*) of around 5%.

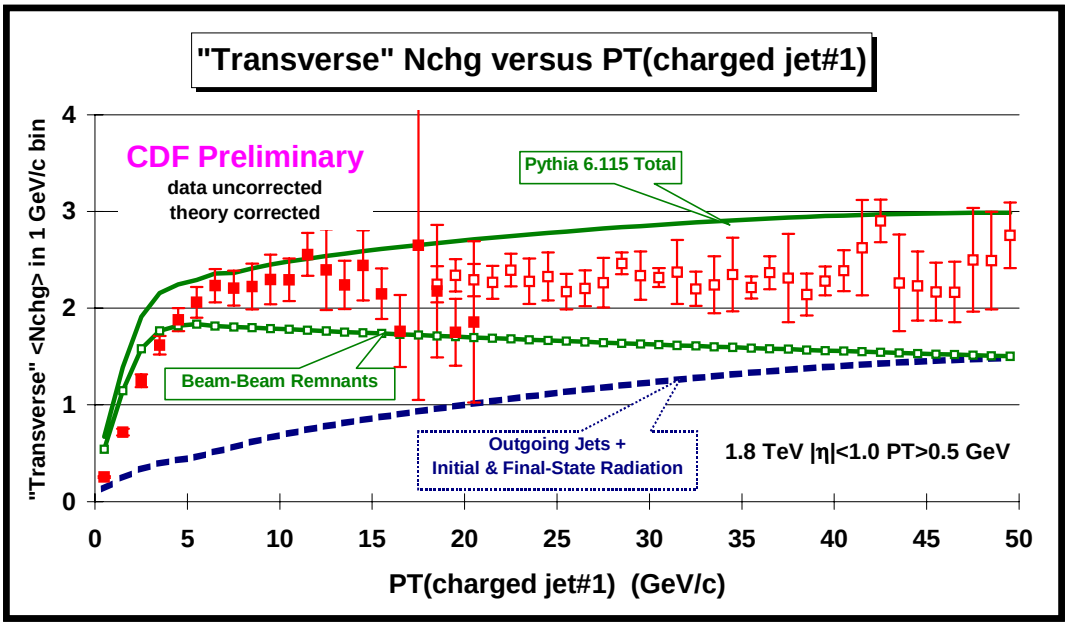

Fig. 3.7. Data on the average number of charged particles (P_T > 0.5 GeV/c and |η| < 1) as a function of P_T(chgjet#1) (*leading charged jet*) for the "transverse" region defined in Fig. 4.2 compared with the QCD hard scattering Monte-Carlo predictions of PYTHIA 6.115. The predictions of PYTHIA are divided into two categories: charged particles that arise from the break-up of the beam and target (*beam-beam remnants*), and charged particles that result from the outgoing jets plus initial and final-state radiation (*hard scattering component*). For PYTHIA the beam-beam remnants include contributions from multiple parton scattering. The theory curves are corrected for the track finding efficiency and have an error (*statistical plus systematic*) of around 5%.

We expect the "transverse" region to be composed predominately from particles that arise from the break-up of the beam and target and from initial-state radiation. This is clearly the case as can be seen in Fig. 3.5 where the predictions of ISAJET for the "transverse" region are divided into three categories: beam-beam remnants, initial-state radiation, and outgoing jets plus final-state radiation. It is interesting to see that it is the beam-beam remnants that are producing the approximately constant "plateau". The contributions from initial-state radiation and from the outgoing hard scattering jets both increase as P_T(chgjet#1) increases. In fact, for ISAJET it is the sharp rise in the initial-state radiation component that is causing the disagreement with the data for P_T(chgjet#1) > 20 GeV/c.

For PYTHIA it makes no sense to distinguish between particles that arise from initial-state radiation from those that arise from final-state radiation, but one can separate the "hard scattering component" from the beam-beam remnants. Also, for PYTHIA the beam-beam remnants include contributions from multiple parton scattering. Fig. 3.6 and Fig. 3.7 compare the "transverse" <Nchg> with the QCD "hard scattering" Monte-Carlo predictions of HERWIG and PYTHIA 6.115, respectively. Here the predictions are divided into two categories: charged particles that arise from the break-up of the beam and target (*beam-beam remnants*), and charged particles that result from the outgoing jets plus initial and final-state radiation (*hard scattering component*). As was the case with ISAJET the beam-beam remnants form the approximately constant "plateau" and the hard scattering component increase as P_T(chgjet#1) increases. However, the hard scattering component of HERWIG and PYTHIA does not rise nearly as fast as the hard scattering component of ISAJET. This difference is due in part to fragmentation

schemes. ISAJET uses independent fragmentation, which produces too many soft hadrons when partons begin to overlap. Another reason for the difference arises from the way the QCD Monte-Carlo produce "parton showers". ISAJET uses a leading-log picture in which the partons within the shower are ordered according to their invariant mass. HERWIG and PYTHIA modify the leading-log picture to include "color coherence effects" which leads to "angle ordering" within the parton shower. Angle ordering produces less high P_T radiation within a parton shower.

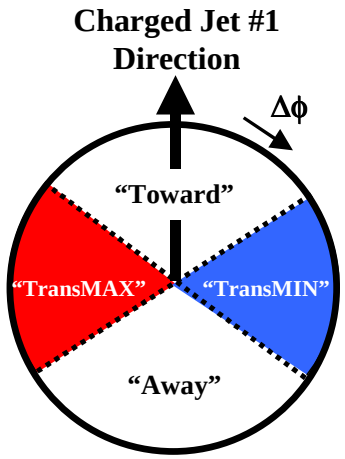

Fig. 4.1. Illustration of correlations in azimuthal angle $\Delta\phi$ relative to the direction of the leading charged jet in the event, chgjet#1. The angle $\Delta\phi = \phi - \phi_{chgjet\#1}$ is the relative azimuthal angle between charged particles and the direction of chgjet#1. On an event by event basis, we define "transMAX" ("transMIN") to be the maximum (minimum) of the two "transverse" pieces, $60^o < \Delta\phi < 120^o$ and $60^o < -\Delta\phi < 120^o$. "TransMAX" and "transMIN" each have an area in η-ϕ space of $\Delta\eta \times \Delta\phi = 2 \times 60^o$. The sum of "TransMAX" and "transMIN" is the total "transverse" region defined in Fig. 3.2.

IV. Maximum and Minimum "Transverse" Regions

We now break up the "transverse" region defined in Fig. 3.2 into two pieces. As illustrated in Fig. 4.1, on an event by event basis, we define "transMAX" ("transMIN") to be the maximum (minimum) of the two "transverse" pieces, $60^o < \Delta\phi < 120^o$ and $60^o < -\Delta\phi < 120^o$. "TransMAX" and "transMIN" each have an area in η-ϕ space of $\Delta\eta \times \Delta\phi = 2 \times 60^o$ and what we previously referred to as the "transverse" region is the sum of "transMAX" and "transMAX". One expects that "transMAX" will pick up more of the initial and final state radiation while "transMIN" should be more sensitive to the beam-beam remnant component of the underlying event. This idea was suggested by Jon Pumplin [5] and used by Valeria Tano [6] in her analysis of maximum and minimum transverse cones (R = 0.7).

Fig. 4.2 shows the data on the $<N_{chg}>$ for the "transMAX" and "transMIN" region as a function of the P_T(chgjet#1) and Fig. 4.3 shows the average difference between the "transMAX" and "transMIN" region. Fig. 4.4 and Fig 4.5 show the same thing for <PTsum>.

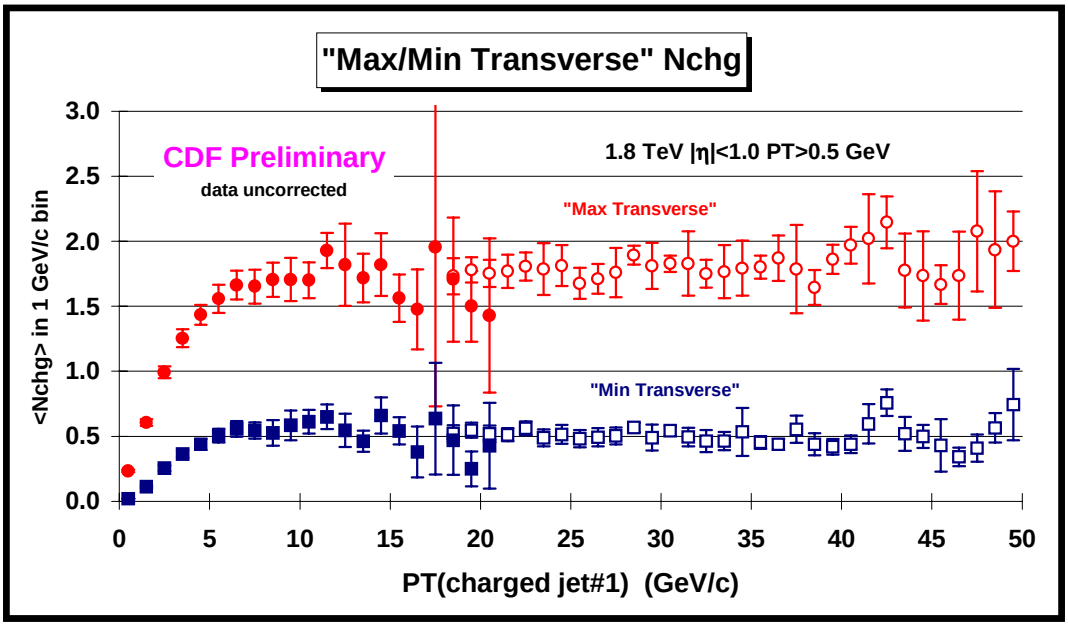

Fig. 4.2. The average number of "transMAX" and "transMIN" charged particles (P_T > 0.5 GeV/c, |η| < 1) as a function of the transverse momentum of the leading charged jet. Each point corresponds to the <Nchg> in a 1 GeV/c bin. The solid (open) points are the Min-Bias (JET20) data. The errors on the (*uncorrected*) data include both statistical and correlated systematic uncertainties. The "transMAX" and "transMIN" regions are defined in Fig. 4.1 and the sum of the two corresponds to the total "transverse" region defined in Fig. 3.2 and shown in Fig. 3.3.

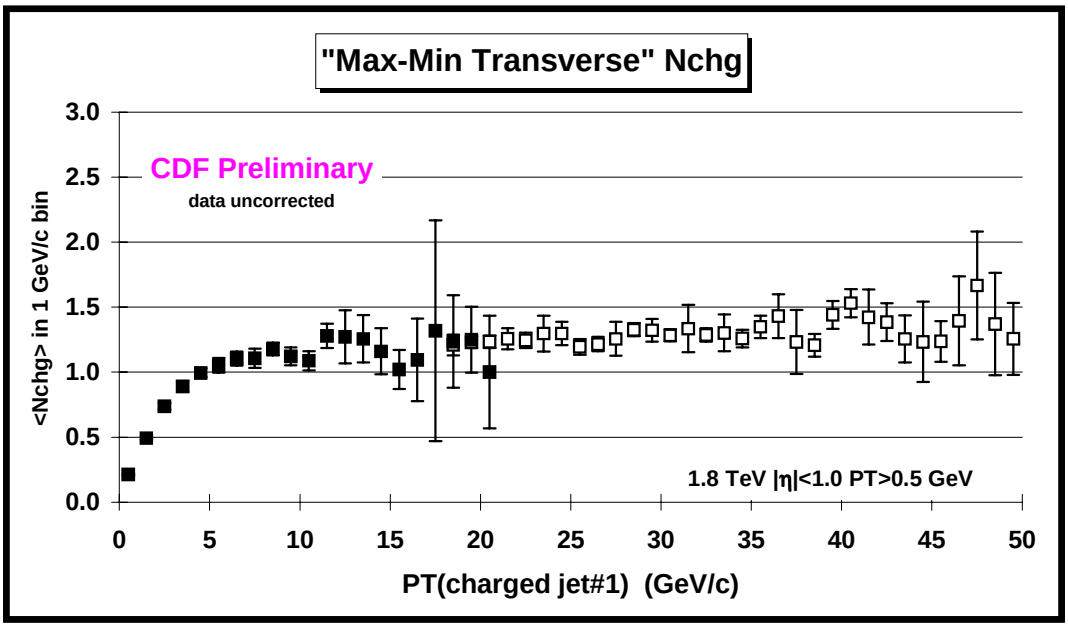

Fig. 4.3. The average difference, "transMAX" minus "transMIN", for the number of charged particles (P_T > 0.5 GeV/c, |η| < 1) as a function of the transverse momentum of the leading charged jet. The solid (open) points are the Min-Bias (JET20) data. The errors on the (*uncorrected*) data include both statistical and correlated systematic uncertainties. The "transMAX" and "transMIN" regions are defined in Fig.4.1.

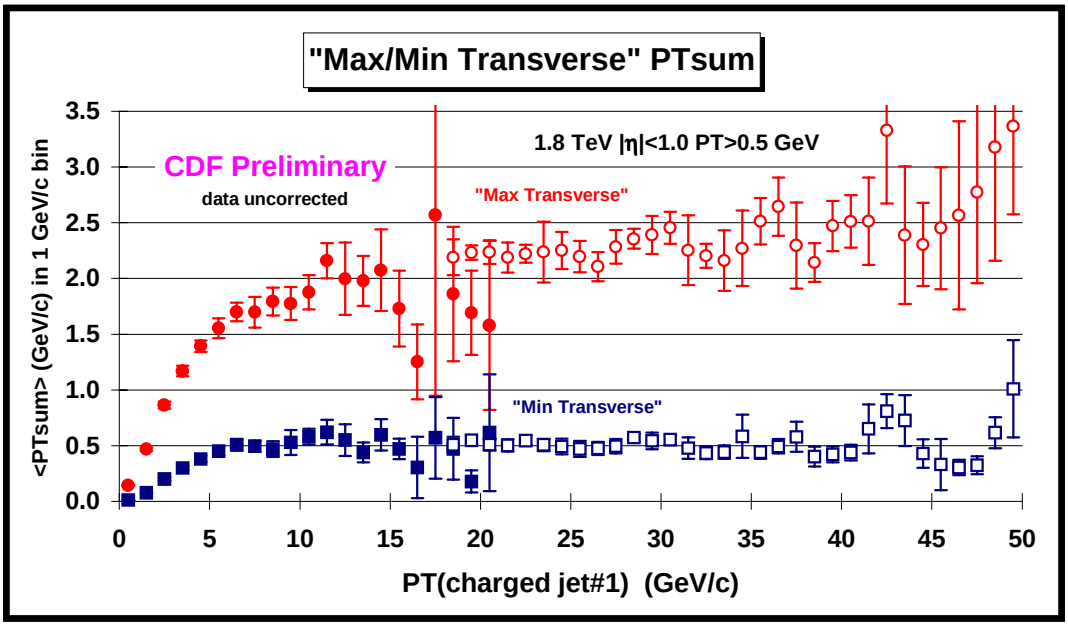

Fig. 4.4. The average scalar P_T sum for "transMAX" and "transMIN" charged particles ($P_T > 0.5$ GeV/c, $|\eta| < 1$) as a function of the transverse momentum of the leading charged jet. Each point corresponds to the <PTsum> in a 1 GeV/c bin. The solid (open) points are the Min-Bias (JET20) data. The errors on the (*uncorrected*) data include both statistical and correlated systematic uncertainties. The "transMAX" and "transMIN" regions are defined in Fig. 4.1 and the sum of the two corresponds to the total "transverse" region defined in Fig. 3.2 and shown in Fig. 3.4.

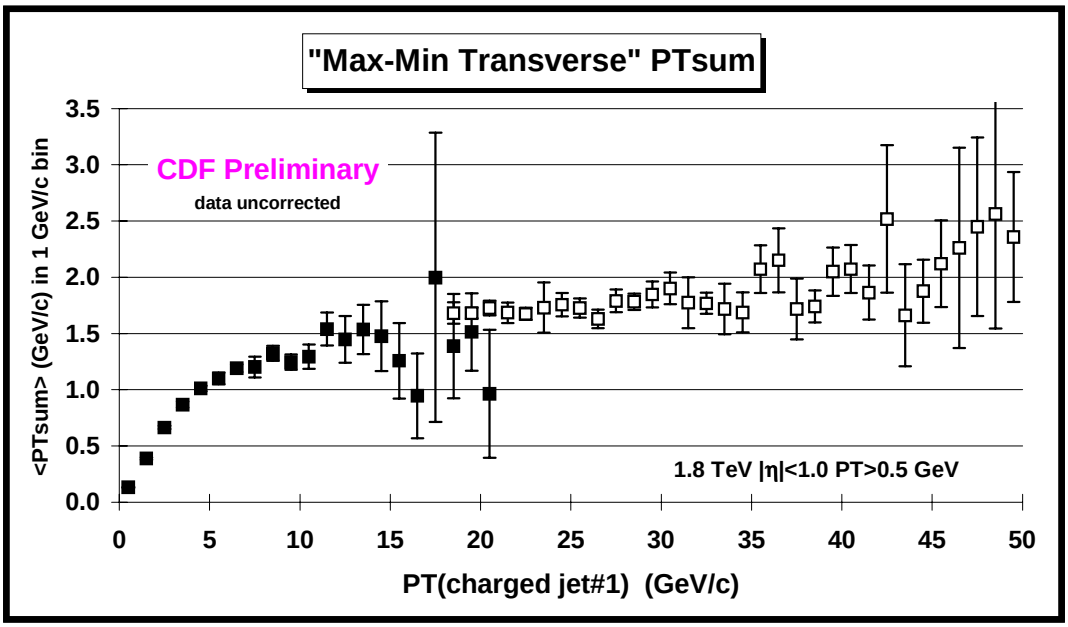

Fig. 4.5. The average difference, "transMAX" minus "transMIN", for the scalar P_T sum of charged particles ($P_T > 0.5$ GeV/c, $|\eta| < 1$) as a function of the transverse momentum of the leading charged jet. The solid (open) points are the Min-Bias (JET20) data. The errors on the (*uncorrected*) data include both statistical and correlated systematic uncertainties. The "transMAX" and "transMIN" regions are defined in Fig.4.1.

Fig. 4.6 and Fig. 4.7 compares the data on the "transMAX/MIN" <Nchg> and <PTsum>, respectively, with the QCD hard scattering Monte-Carlo models of ISAJET and HERWIG. The excess of charged particles produced by ISAJET in the "transverse" region seen in Fig. 3.5 occurs in both "transMAX" and "transMIN". Fig. 4.8, Fig. 4.9, and Fig. 4.10 are similar to Fig. 3.5 but for "transMAX", "transMIN", and the difference. In these plots the predictions of ISAJET are divided into three categories: beam-beam remnants, initial-state radiation, and outgoing jets plus final-state radiation. Again we see that the reason ISAJET overshoots the data is due to too many charged particles from initial state radiation. One must use caution when comparing to the difference of "transMAX" and "transMIN". ISAJET does a reasonable job at fitting the difference in Fig. 4.10, but overshoots greatly on the sum of "transMAX" and "transMIN" (Fig. 3.5).

Fig. 4.11, Fig. 4.12, and Fig. 4.13 are similar to Fig. 3.6 but for "transMAX", "transMIN", and the difference. Here the predictions of HERWIG are divided into two categories: charged particles that arise from the break-up of the beam and target (*beam-beam remnants*), and charged particles that result from the outgoing jets plus initial and final-state radiation (*hard scattering component*). It is clear from these plots that "transMAX" is more sensitive to the hard scattering component of the underlying event while "transMIN" is more sensitive to the beam-beam remnants. For HERWIG at P_T(chgjet#1) = 40 GeV/c the hard scattering component makes up 62% of the "transMAX" <Nchg> with 38% coming from the beam-beam remnants. On the other hand, the hard scattering component makes up only 42% of the "transMIN" <Nchg> with 58% coming from the beam-beam remnants at P_T(chgjet#1) = 40 GeV/c. Taking difference between "tansMAX" and "transMIN" does not completely remove the beam-beam remnant component, but reduces it to only about 32% at P_T(chgjet#1) = 40 GeV/c.

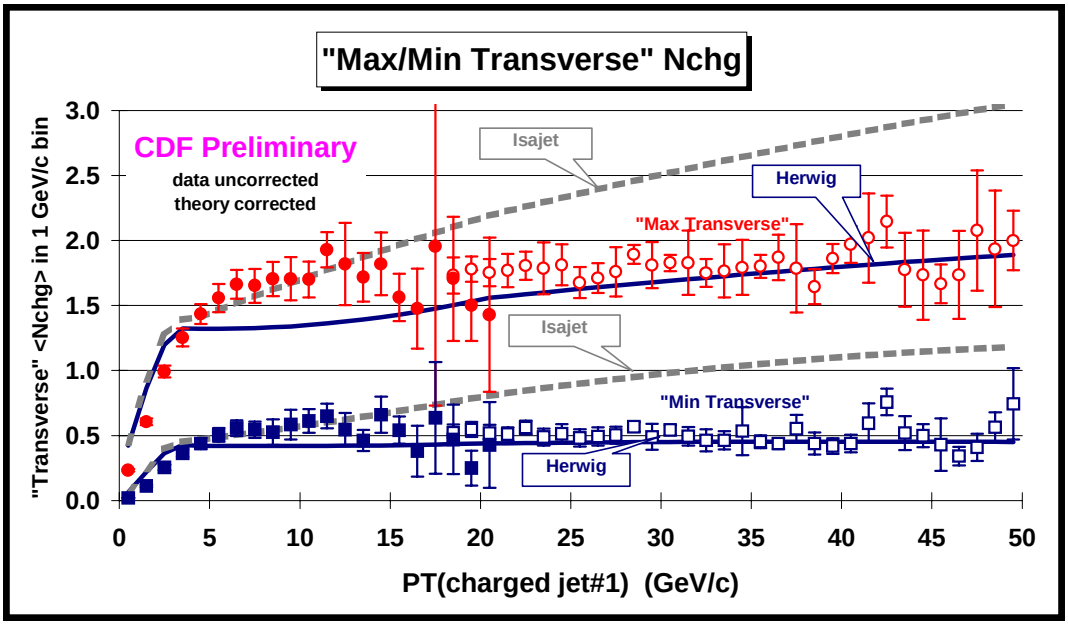

Fig. 4.6. Data from Fig. 4.2 on he average number of "transMAX" and "transMIN" charged particles (P_T > 0.5 GeV/c, |η| < 1) as a function of the transverse momentum of the leading charged jet compared with the QCD hard scattering Monte-Carlo models of ISAJET and HERWIG. The theory curves are corrected for the track finding efficiency and have an error (*statistical plus systematic*) of around 5%.

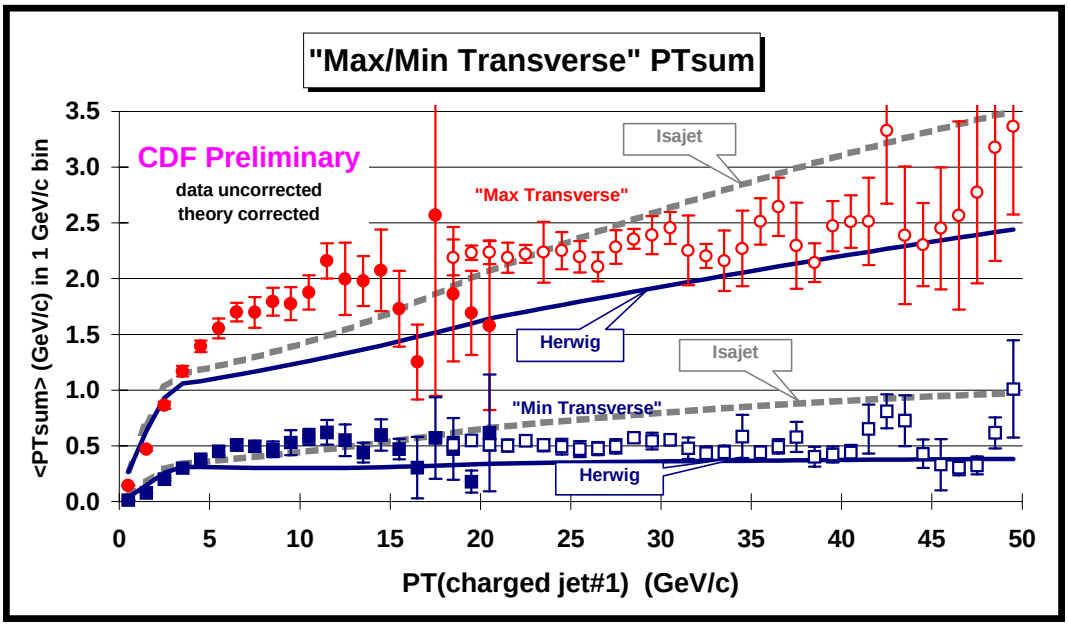

Fig. 4.7. Data from Fig. 4.4 on he average scalar P_T sum of "transMAX" and "transMIN" charged particles ($P_T > 0.5$ GeV/c, $|\eta| < 1$) as a function of the transverse momentum of the leading charged jet compared with the QCD hard scattering Monte-Carlo models of ISAJET and HERWIG. The theory curves are corrected for the track finding efficiency and have an error (*statistical plus systematic*) of around 5%.

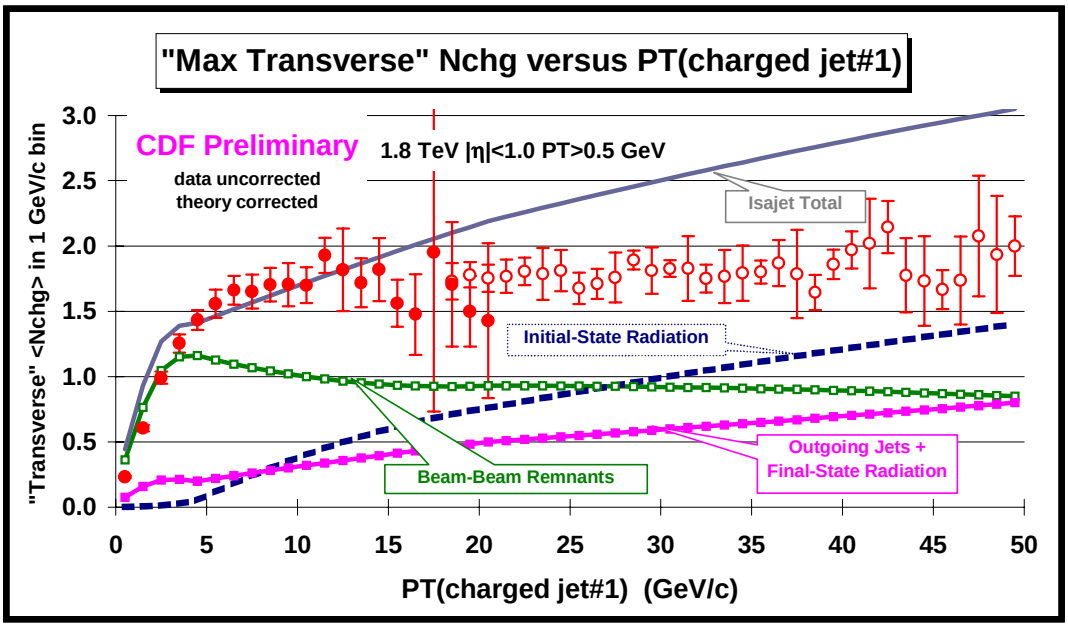

Fig. 4.8. Data from Fig. 4.2 on the average number of "transMAX" charged particles ($P_T > 0.5$ GeV/c and $|\eta| < 1$) as a function of P_T(chgjet#1) (*leading charged jet*) compared with the QCD hard scattering Monte-Carlo predictions of ISAJET. The predictions of ISAJET are divided into three categories: charged particles that arise from the break-up of the beam and target (*beam-beam remnants*), charged particles that arise from initial-state radiation, and charged particles that result from the outgoing jets plus final-state radiation (see Fig. 1.1). The theory curves are corrected for the track finding efficiency and have an error (*statistical plus systematic*) of around 5%.

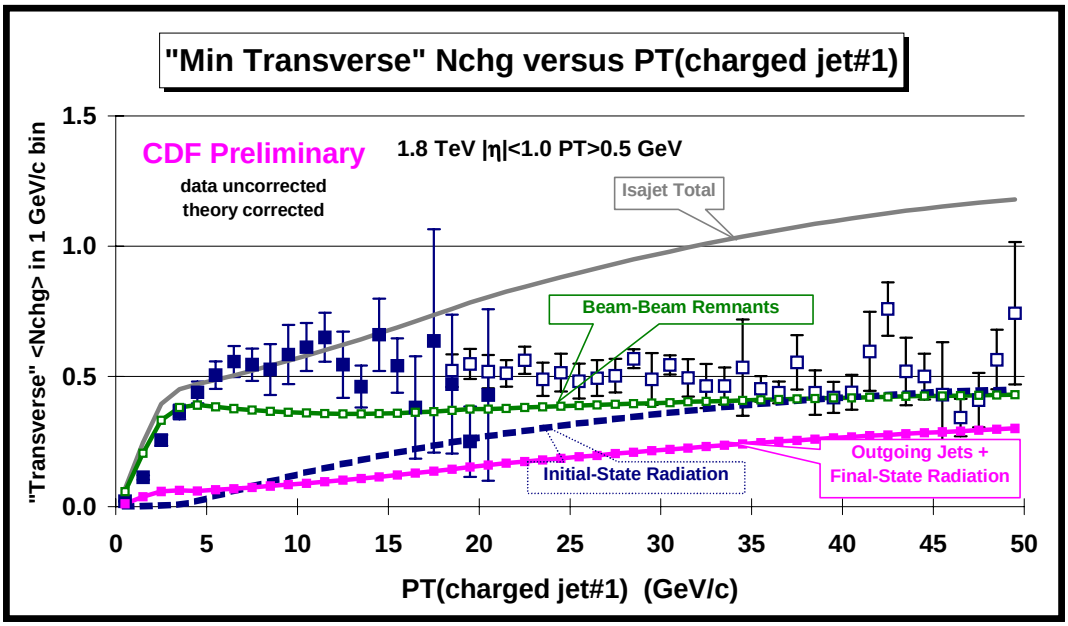

Fig. 4.9. Data from Fig. 4.2 on the average number of "transMIN" charged particles (P_T > 0.5 GeV/c and |η| < 1) as a function of P_T(chgjet#1) (*leading charged jet*) compared with the QCD hard scattering Monte-Carlo predictions of ISAJET. The predictions of ISAJET are divided into three categories: charged particles that arise from the break-up of the beam and target (*beam-beam remnants*), charged particles that arise from initial-state radiation, and charged particles that result from the outgoing jets plus final-state radiation (see Fig. 1.1). The theory curves are corrected for the track finding efficiency and have an error (*statistical plus systematic*) of around 5%.

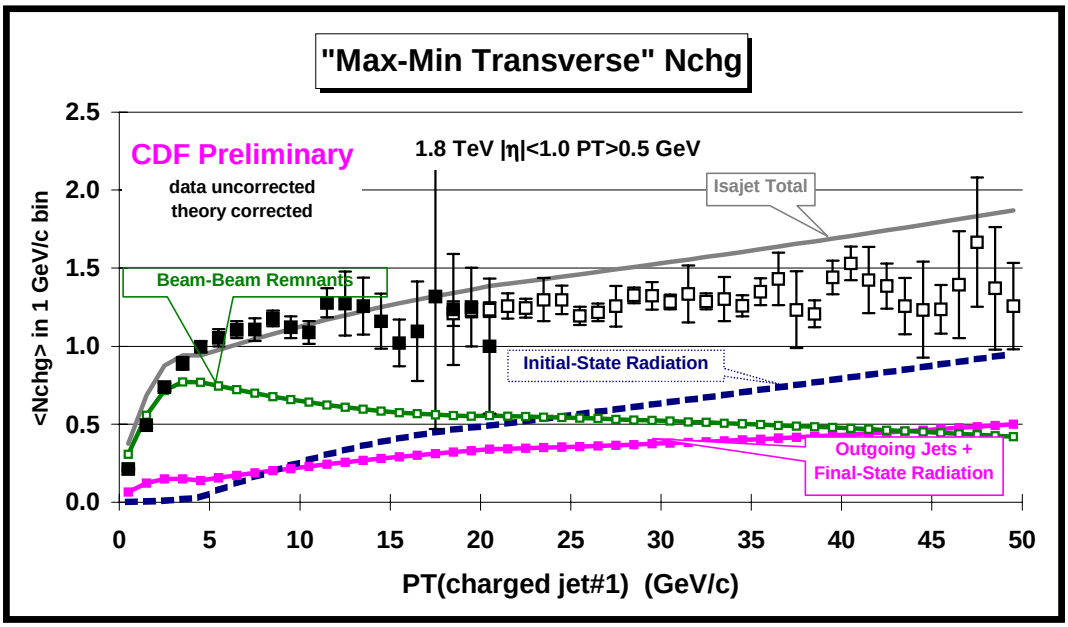

Fig. 4.10. Data from Fig. 4.3 on the average difference, "transMAX" minus "transMIN", for the number of charged particles (P_T > 0.5 GeV/c and |η| < 1) as a function of P_T(chgjet#1) (*leading charged jet*) compared with the QCD hard scattering Monte-Carlo predictions of ISAJET. The predictions of ISAJET are divided into three categories: charged particles that arise from the break-up of the beam and target (*beam-beam remnants*), charged particles that arise from initial-state radiation, and charged particles that result from the outgoing jets plus final-state radiation (see Fig. 1.1). The theory curves are corrected for the track finding efficiency and have an error (*statistical plus systematic*) of around 5%.

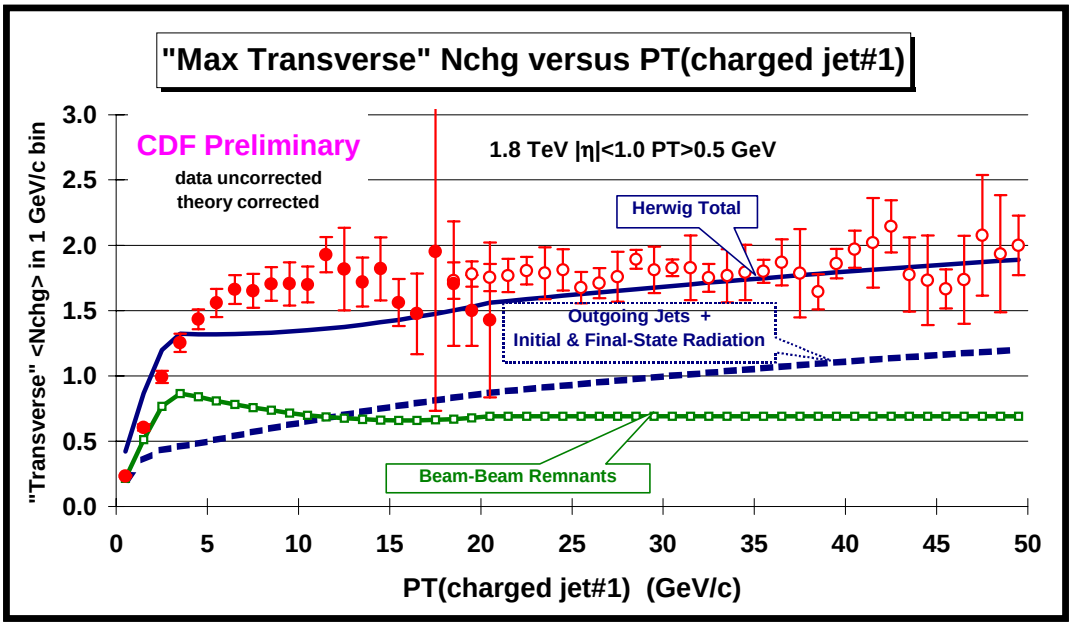

Fig. 4.11. Data from Fig. 4.2 on the average number of "transMAX" charged particles (P_T > 0.5 GeV/c and |η| < 1) as a function of P_T(chgjet#1) (*leading charged jet*) compared with the QCD hard scattering Monte-Carlo predictions of HERWIG. The predictions of HERWIG are divided into two categories: charged particles that arise from the break-up of the beam and target (*beam-beam remnants*), and charged particles that result from the outgoing jets plus initial and final-state radiation (*hard scattering component*) (see Fig. 1.1). The theory curves are corrected for the track finding efficiency and have an error (*statistical plus systematic*) of around 5%.

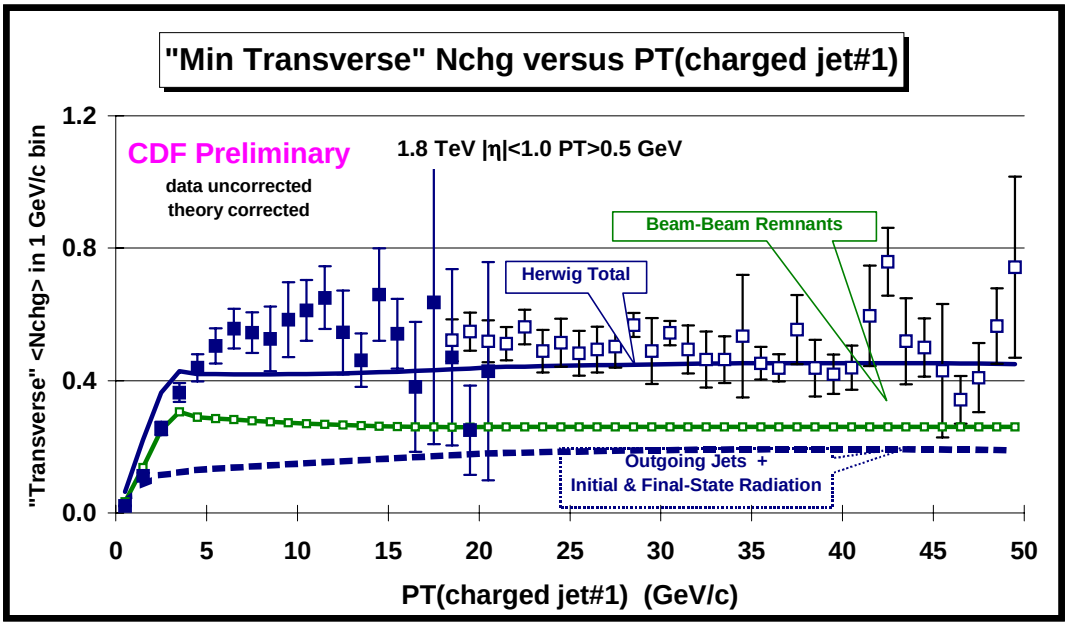

Fig. 4.12. Data from Fig. 4.2 on the average number of "transMIN" charged particles (P_T > 0.5 GeV/c and |η| < 1) as a function of P_T(chgjet#1) (*leading charged jet*) compared with the QCD hard scattering Monte-Carlo predictions of HERWIG. The predictions of HERWIG are divided into two categories: charged particles that arise from the break-up of the beam and target (*beam-beam remnants*), and charged particles that result from the outgoing jets plus initial and final-state radiation (*hard scattering component*) (see Fig. 1.1). The theory curves are corrected for the track finding efficiency and have an error (*statistical plus systematic*) of around 5%.

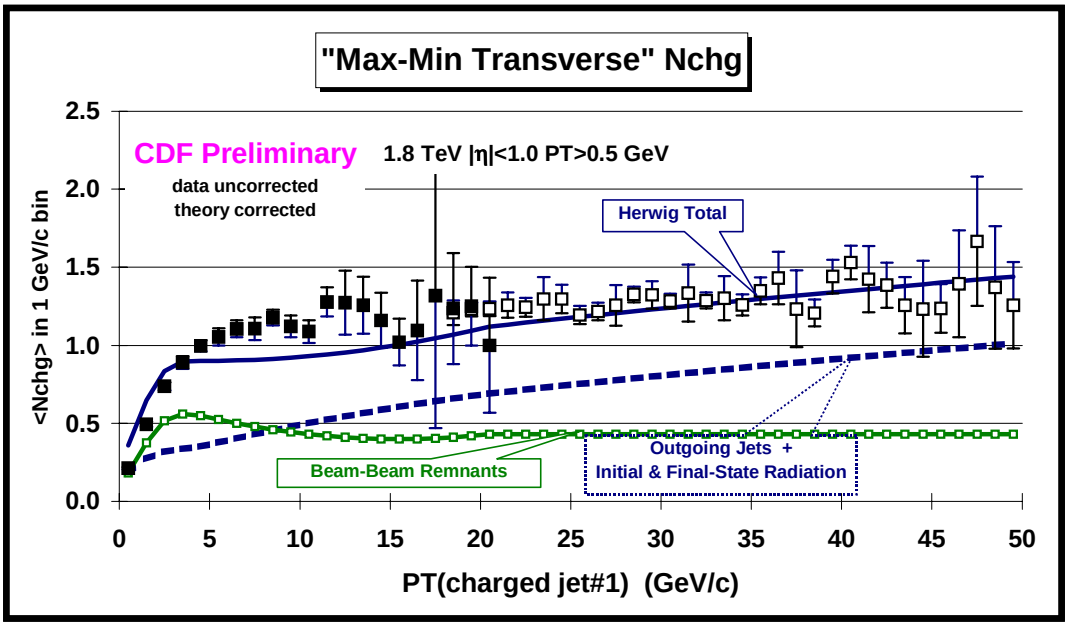

Fig. 4.13. Data from Fig. 4.3 on the average number of "transMIN" charged particles (P_T > 0.5 GeV/c and |η| < 1) as a function of P_T(chgjet#1) (*leading charged jet*) compared with the QCD hard scattering Monte-Carlo predictions of HERWIG. The predictions of HERWIG are divided into two categories: charged particles that arise from the break-up of the beam and target (*beam-beam remnants*), and charged particles that result from the outgoing jets plus initial and final-state radiation (*hard scattering component*) (see Fig. 1.1). The theory curves are corrected for the track finding efficiency and have an error (*statistical plus systematic*) of around 5%.

V. Summary and Conclusions

Clearly studying the "transMAX" and "transMIN" pieces of the "transverse" region provides additional information not contained in the sum. The various components that make up the underlying event are weighted differently in "transMAX" and "transMIN" terms. The "transMAX" term preferentially selects the hard component of the underlying event (*outgoing jets plus initial and final-state radiation)* while the "transMIN" term preferentially selects the beam-beam remnant component. Unfortunately one cannot cleanly isolate a single component of the underlying since all components contribute to both "transMAX", "transMIN", and to the difference. However, requiring the QCD hard scattering Monte-Carlo models to fit both "transMAX" and "transMIN" (or the sum and difference) puts additional constraints on the way the generators model the underlying event.

We plan to tune the QCD Monte-Carlo models to describe more accurately the underlying event in hard scattering processes and the "transMAX/MIN" observables will play and important role in this procedure.

References and Footnotes

1. *Charged Jet Evolution and the Underlying Event in Proton-Antiproton Collisions at 1.8 TeV*, Rick Field and David Stuart, CDF/PUB/CDF/CDFR/5453. *The Underlying Event in Large Transverse Momentum Charged Jet and Z-boson Production*, Rick Field, CDF/PUB/MIN_BIAS/PUBLIC/5463. *The Underlying Event: Dijet vs. Z-jet*, Rick Field, Richard Haas, Henry Frisch, and David Stuart, CDF/ANAL/CDF/CDFR/5295.

2. T. Sjostrand, Phys. Lett. **157B**, 321 (1985); M. Bengtsson, T. Sjostrand, and M. van Zijl, Z. Phys. **C32**, 67 (1986); T. Sjostrand and M. van Zijl, Phys. Rev. **D36**, 2019 (1987).

3. G. Marchesini and B. R. Webber, Nucl. Phys **B310**, 461 (1988); I. G. Knowles, Nucl. Phys. B310, 571 (1988); S. Catani, G. Marchesini, and B. R. Webber, Nucl. Phys. **B349**, 635 (1991).

4. F. Paige and S. Protopopescu, BNL Report, BNL38034, 1986 (unpublished), version 7.32.

5. *Hard Underlying Event Corrections to Inclusive Jet Cross-Sections*, Jon Pumplin, Phys. Rev. **D57**, 5787 (1998).

6. *Comparison of Soft Momentum Distribution in CDF data and HERWIG+QFL at 1800 and 630 GeV*, Anwar Bhatti, Eve Kovacs, Joey Huston, and Valeria Tano, CDF/ANAL/JET/CDFR/5600. *Comparison of Underlying Event Energy in HERWIG and CDF Data*, Anwar Bhatti, Joey Huston, Eve Kovacs, and Valeria Tano, CDF/ANAL/JET/CDFR/5214.